WALAILAK JOURNAL
http://wjst.wu.ac.th Physical Sciences

Investigation of Electron Crystallization in a HCP Structure

Ratnavelu RAJESWARAPALANICHAMY[1,*], Arjunan MURUGAN[1], Shunmugam KANAGAPRABHA[2], Shanmugam PUVANESWARI[3] and Kombiah IYAKUTTI[4]

[1]*Department of Physics, Nadar Mahajana Sangam S. Vellaichamy Nadar College, Madurai, Tamilnadu 625019, India*
[2]*Department of Physics, Kamaraj College, Tuticorin, Tamilnadu 628003, India*
[3]*Department of Physics, E. M. G. Yadhava Women's College, Madurai, Tamilnadu 625014, India*
[4]*Noorul Islam University, Kanyakumari, Tamilnadu 629180, India*

([*]Corresponding author's e-mail: rrpalanichamy@gmail.com)

Received: 20 February 2012, Revised: 15 September 2012, Accepted: 4 June 2013

Abstract

The ground state energies of non-magnetic, ferromagnetic and antiferromagnetic phases of 3D electron crystals corresponding to hcp structure are computed. In each case, the possibility of the Wigner electrons having cubic or spherical constant energy surface (the region of integration in momentum space) is investigated. The role of correlation energy is suitably taken into account. The range of the low density region favourable for Wigner electron crystallization is found. The structure dependent Wannier functions, which give proper localized representation for the Wigner electrons in the crystal, are employed in the calculation.

Keywords: Electron crystal, Wannier function, magnetism, Yukawa type background, correlation energy

Introduction

In 1934, Wigner [1,2] suggested that an electronic assembly will crystallize in to an electron crystal in a uniform neutralizing positive background. Edwards and Hillel [3] have used a variational approach to the Hartree-Fock approximation and the corresponding orbitals are the Bloch states. Later Hedin [4] and in more detail Misawa [5] used the Gell-Mann-Brueckner [6] formalism to compute the tendency towards the ferromagnetism. The basic quantity, r_s is a convenient indicator of the electron density, which is a dimensionless parameter. It is defined as the radius of the unit sphere enclosing volume equal to the volume per electron of the electron gas. Misawa [5] found that ferromagnetism could occur for $r_s > 10$. Mott [7] predicted that, the transition from ferromagnetic gas to ferromagnetic crystal is at $r_s \approx 20$. Carr [8] and Edwards and Hillel [3] investigated the ferromagnetic and antiferromagnetic states of the Wigner electron crystal. Young *et al.* [9] experimentally found weak ferromagnetism in the low density electron crystal at high temperature. Caperley [10] explained the ferromagnetism of electron gas at low density using a Quantum Monte Carlo method. His calculation predicted that the electrons will spin align at a density less than 2×10^{20} cm^{-3} and crystallize at a density 2×10^{18} cm^{-3}. The Hartree-Fock ground state of the three dimensional electron gas was investigated by Zhang and Caperley [11]. Paplavskyy *et al.* [12] studied the local density of states of the electron crystal in graphene. Wigner electron crystallization in two dimensional amorphous dielectric materials was investigated [13]. Campbell *et al.* [14] have produced the laser cooled Wigner crystals of ^{229}Th for optical excitation of the nuclear isomer. Recently, we have investigated the Wigner crystallization of quadratically dispersed electrons

in graphene [15]. In this work, the ground state energies of the non-magnetic, ferromagnetic and antiferromagnetic phases of 3D Wigner electron crystal with uniform neutralizing and Yukawa type positive backgrounds with hcp structure are computed. The crystallization density is calculated.

Theory

The Wannier functions are constructed using the variational principle given by Koster-Kohn [16,17]. In this work, we transform the Gaussians into orthogonalized atomic orbitals using the method given by Lowdin [18] and Calais and Appel [19]. The Wannier function thus obtained is;

$$W(\mathbf{r}) = \sum_{m} \phi(\mathbf{m},\mathbf{r}) \Delta^{-1/2}(\mathbf{m},0) \tag{1}$$

where $\phi(\mathbf{m},\mathbf{r})$ is the Gaussian function and $\Delta^{-1/2}(\mathbf{m},0)$ is the reciprocal square root of the overlap matrix. The expression for $\Delta^{-1/2}(\mathbf{m},0)$ is [19,20].

$$\Delta^{-1/2}(\mathbf{m},0) = V_{oa} \int \frac{\cos 2\pi \mathbf{k}.\mathbf{m}}{[d(k)]^{1/2}} d\mathbf{k} \tag{2}$$

where V_{oa} is the volume per electron and;

$$d(\mathbf{k}) = 1 + 2\sum_{m} s(\mathbf{m}) \cos(2\pi \mathbf{k}.\mathbf{m}) \tag{3}$$

and $s(\mathbf{m})$ is the overlap integral, **k** is the reciprocal lattice vector and **m** is the lattice vector in ordinary space.

We can transform Eq. (2) for different cubic structures. If ψ are Bloch orbitals of the state under consideration, then the Wannier function W and ψ are related by;

$$W = \psi\, U^{+}, \qquad \psi = WU \tag{4}$$

with

$$U(\mathbf{m},\mathbf{k}) = \frac{1}{\sqrt{N}} \exp(2\pi i \mathbf{k}.\mathbf{m}) \tag{5}$$

We have considered the non-magnetic (NC), ferromagnetic (FC) and antiferromagnetic (AC) phases of the 3D electron crystal. Like Edwards and Hillel [3], we have;

$$\rho_{NC}(\mathbf{x},\mathbf{x}') = \rho_{NC}(\mathbf{r},\mathbf{r}')[\alpha\alpha' + \beta\beta'] \tag{6}$$

$$\rho_{FC}(\mathbf{x},\mathbf{x}') = \rho_{FC}(\mathbf{r},\mathbf{r}')\,\alpha\alpha' \tag{7}$$

$$\rho_{AC}(\mathbf{x},\mathbf{x}') = \rho^{+}_{AC}(\mathbf{r},\mathbf{r}')\alpha\alpha' + \rho^{-}_{AC}(\mathbf{r},\mathbf{r}')\beta\beta' \tag{8}$$

where $\alpha\alpha$' and $\beta\beta'$ represent the spin of the electrons and in terms of the Wannier function.

$$\rho_{NC}(\mathrm{r},\mathrm{r}') = \sum_{\mathrm{m},\mathrm{m}'} W_{NC}(\mathbf{m},\mathbf{r})\, R_{NC}(\mathbf{m},\mathbf{m}')\, W^{*}_{NC}(\mathbf{m}',\mathbf{r}') \tag{9}$$

$$\rho_{FC}(\mathbf{r},\mathbf{r}') = \sum_{m,m'} W_{FC}(\mathbf{m},\mathbf{r})\, R_{FC}(\mathbf{m},\mathbf{m}')\, W_{FC}{}^{*}(\mathbf{m}',\mathbf{r}') \tag{10}$$

$$\rho^{\pm}_{AC}(\mathrm{r},\mathrm{r}') = \sum_{\mathrm{m},\mathrm{m}'} W_{NC}(\mathbf{m},\mathbf{r})\, R^{\pm}_{AC}(\mathbf{m},\mathbf{m}')\, W^{*}_{NC}(\mathbf{m}',\mathbf{r}') \tag{11}$$

we have;

$$R_{NC}(\mathbf{m},\mathbf{m}') = V_{oa} \int_{k_{NC}} \exp[2\pi\, i\mathbf{k}.(\mathbf{m}-\mathbf{m}')]\, d\mathbf{k} \tag{12}$$

and is similar for the FC while a special case is needed for AC. We further notice that;

$$\int \rho_{NC}(\mathbf{r},\mathbf{r}')d\mathbf{r} = \mathrm{N}/2 \tag{13}$$

$$\int \rho_{FC}(\mathbf{r},\mathbf{r}')d\mathbf{r} = \mathrm{N} \tag{14}$$

$$\int \rho_{AC}(\mathbf{r},\mathbf{r}')d\mathbf{r} = \mathrm{N}/2 \tag{15}$$

In the calculation of the R_j (j = NC, FC, AC), we can take the region of integration in k-space as a cubic or spherical surface. Now, we consider the NC and FC cases.
From Eq. (13) we can write;

$$\sum_{\mathbf{m}} \mathrm{R_{NC}}(\mathbf{m},\mathbf{m}) = \frac{\mathrm{N}}{2} \tag{16}$$

Similarly, from Eq. (14) we can write;

$$\sum_{\mathbf{m}} \mathrm{R_{FC}}(\mathbf{m},\mathbf{m}) = \mathrm{N} \tag{17}$$

Combining Eq. (12) with the above equations and integrating over a cube gives;

$$\mathrm{R_j^C}(\mathbf{m},\mathbf{m}') = \mathrm{V_{oa}} \prod_{\mathrm{i=1}}^{3} \frac{\sin \pi\ \mathrm{b_j}\left|\mathrm{m_i} - \mathrm{m_i'}\right|}{\pi\left|\mathrm{m_i} - \mathrm{m_i'}\right|} \tag{18}$$

where $\mathrm{b_j}$ is the cube edge of the cubic surface. Integrating over a sphere gives;

$$\mathrm{R_j^S}(\mathbf{m},\mathbf{m}') = \left(\frac{4\pi}{3}\right)\mathrm{k_j}^3\ \mathrm{V_{oa}}\ \mathrm{q}\left(2\pi\,\mathrm{k_j}\left|\mathbf{m}-\mathbf{m}'\right|\right) \tag{19}$$

where

$$q(x) = \frac{3(\sin x - x\cos x)}{x^3} \tag{20}$$

and

$$x = 2\pi\,\mathrm{k_j}(\mathbf{m}-\mathbf{m}') \tag{21}$$

where $\mathrm{k_j}$ is the radius of the spherical surface in k-space. Combining Eqs. (12) and (16), we get;

$$\mathrm{V_{NC}} = \frac{1}{2\,\mathrm{V_{oa}}} \tag{22}$$

Similarly for the FC case

$$\mathrm{V_{FC}} = \frac{1}{\mathrm{V_{oa}}} \tag{23}$$

For a hcp lattice, $V_{oa} = a^3/6$, where 'a' is the cube edge. Thus, a cubic surface in k-space has the cube edge.

$$b_{NC} = \frac{3^{1/3}}{a} \tag{24}$$

and $$b_{FC} = \frac{6^{1/3}}{a} \tag{25}$$

The radius of the spherical surface in k-space is;

$$k_{NC} = \left(\frac{9}{4\pi}\right)^{1/3} \frac{1}{a} \tag{26}$$

and

$$k_{FC} = \left(\frac{9}{2\pi}\right)^{1/3} \frac{1}{a} \tag{27}$$

Effect of positive background

The Hartree-Fock effective operator for a normal system is;

$$H_{eff}(1) = \frac{1}{2}\Delta_1 - \sum_g \frac{Z_g}{|\mathbf{r}_1 - R_g|} + \int \frac{(1-P_{12})\rho(\mathbf{x}_2, \mathbf{x}_2')}{r_{12}} d\mathbf{x_2} \tag{28}$$

For any extended system one has to evaluate carefully the matrix elements of the long range electrostatic part.

$$V_C(\mathbf{r}_1) = -\sum_g \frac{Z_g}{|\mathbf{r}_1 - R_g|} + \int \frac{\rho(\mathbf{x}_2, \mathbf{x}_2')}{r_{12}} d\mathbf{x}_2 \tag{29}$$

so that the large parts are cancelled out [18,21-23]. Uniform distribution and point like nuclei are the two extreme cases of positive charge distribution and the entire real situations lie between the above two cases. In the present work, we have investigated both cases.

Uniform neutralizing positive background

For the uniform distribution of positive background, the two terms in Eq. (29) cancel each other and $V_c(\mathbf{r}_1) = 0$. Then, we are left with the kinetic energy term and exchange energy term in H_{eff}. That is;

$$H_{eff}(1) = \frac{1}{2}\Delta_1 - \int \frac{P_{12}\rho(\mathbf{x}_2, \mathbf{x}_2')}{r_{12}} d\mathbf{x}_2 \tag{30}$$

The kinetic energy term and the exchange energy term in Eq. (30) are evaluated using the expressions given by Shavift [24].

Non-uniform positive background

For the Wigner electron crystal, it is reasonable to have a non-uniform distribution of positive charge, which does not have to be uniform. Hall pointed out that the limit of zero for λ yields the Wigner electron crystal. The non-uniform positive background is represented by a periodic array of Yukawa distribution with variable ripple parameter λ.

Yukawa type distribution

The background is represented by a charge distribution centered about each lattice site.

$$\mathrm{P(r)}=\frac{\lambda^{2}}{4\pi}\frac{\exp(-\lambda\,\mathrm{r})}{\mathrm{r}} \tag{31}$$

where λ is the variational parameter.
If we can define;

$$\overline{\rho}(\mathbf{r})=\rho(\mathbf{r})-\mathrm{P}(\mathbf{r}) \tag{32}$$

then the expression for $\mathrm{V_c}(\mathbf{r}_1)$ is;

$$\mathrm{V_c}(\mathbf{r}_1)=\frac{1}{2}\int\frac{\overline{\rho}(\mathbf{r}_2)}{\mathrm{r}_{12}}d\mathbf{r}_2 . \tag{33}$$

The expression for the electrostatic energy with Yukawa type positive background is derived as;

$$\begin{aligned}\mathrm{E_c}=&\frac{1}{2}\sqrt{\frac{2\alpha}{\pi}}\sum_{\mathbf{m},\mathbf{m}'}\mathrm{R}(\mathbf{m},\mathbf{m}')\mathrm{M}(\mathbf{m},\mathbf{m}')\mathrm{F_0}(\mathbf{PQ}^2)\\&\times\exp\left(-\frac{\alpha}{4}\overline{00}^2-\frac{\alpha}{4}\overline{\mathbf{mm}'}^2\right)+\frac{\lambda}{4}\\&-\sqrt{\frac{4\alpha}{\pi}}\sum_{\mathbf{m},\mathbf{m}'}\mathrm{R}(\mathbf{m},\mathbf{m}')\mathrm{M}(\mathbf{m},\mathbf{m}')\mathrm{F_0}(\alpha\mathbf{CP}^2)\\&\times\exp\left(-\frac{\alpha}{4}\overline{00}^2-\frac{\alpha}{4}\overline{\mathbf{mm}'}^2\right)\\&+4\pi\left(\frac{\alpha}{\pi}\right)^{3/2}\sum_{\mathbf{m},\mathbf{m}'}\mathrm{R}(\mathbf{m},\mathbf{m}')\mathrm{M}(\mathbf{m},\mathbf{m}')\\&\times\int\exp\left(-\frac{\alpha}{2}|\mathbf{r}_2-\mathbf{m}|^2-\frac{\alpha}{2}|\mathbf{r}_2-\mathbf{m}'|^2-\lambda\mathbf{r}_2\right)\times\mathbf{r}_2 d\mathbf{r}_2\end{aligned} \tag{34}$$

where $\mathrm{M}(\mathbf{m},\mathbf{m}')$ is the weight factor depending upon the number of nearest neighbours and $\mathrm{F_o}(\mathrm{t})$ is defined as;

$$\mathrm{F_o(t)}=\frac{1}{2}\sqrt{\frac{\pi}{\mathrm{t}}}\mathrm{erf}(\sqrt{\mathrm{t}}) \tag{35}$$

Antiferromagnetic phase

Consider a system with 2N physically equivalent sites based on a lattice with one site at each lattice point, the lattice consists of two equivalent interpenetrating sub-lattices, the nearest neighbours of any site belonging to the opposite sub-lattice. Such a system is a special case of systems called antiferromagnetic structures [25]. Sites are even or odd depending on their relation to a chosen site, those on the same sub-lattice are even.

If there are 2N electrons in the lattice then each sub-lattice will have N electrons. The first Brillouin zone of the sub lattice contains just N_k vectors, half as many as that of a full lattice. Let the sub-lattice zone be placed symmetrically around zero inside the full lattice, the remaining portion of the full lattice zone is also the second Brillouin zone of the sub-lattice, called a residual zone. For every $\mathbf{K}$ inside the sub-lattice zone, there corresponds a unique conjugate $\mathbf{K}$ in the residual zone, such that the functions;

$$\chi(\mathbf{k}) = \frac{1}{\sqrt{2}}\left[\psi(\mathbf{k}) + \psi(\bar{\mathbf{k}})\right] \tag{36}$$

where $\bar{\mathbf{k}} = \mathbf{k} + \mathbf{K}$, are sub-lattice Bloch type orbitals having density only on a single sub-lattice, $\chi(\mathbf{k})$ being associated with the even lattice and $\bar{\chi}(\mathbf{k})$ with odd sub-lattice. The Fock-Dirac matrices can be constructed as;

$$\rho_{AC}^{+}(\mathbf{r},\mathbf{r}') = \sum_{\mathbf{k}}^{\mathbf{k}_{AC}^{+}} \chi(\mathbf{k},\mathbf{r})\,\chi^{*}(\mathbf{k},\mathbf{r}')$$
$$\rho_{AC}^{-}(\mathbf{r},\mathbf{r}') = \sum_{\mathbf{k}}^{\mathbf{k}_{AC}^{-}} \bar{\chi}(\mathbf{k},\mathbf{r})\,\bar{\chi}^{*}(\mathbf{k},\mathbf{r}) \tag{37}$$

then $\rho_{AC} = \rho_{AC}^{+} + \rho_{AC}^{-}$. In terms of Wannier functions;

$$\rho_{AC} = \frac{1}{2}\sum_{\mathbf{m},\mathbf{m}'} W_{AC}(\mathbf{m},\mathbf{r})\left[R_{AC}^{+} + R_{AC}^{-}\right] W_{AC}^{*}(\mathbf{m}',\mathbf{r}') \tag{38}$$

That is;

$$\rho_{AC}^{+} = \frac{1}{2}\sum_{\mathbf{m},\mathbf{m}'} W_{AC}(\mathbf{m},\mathbf{r})\left[R_{AC}^{+}(\mathbf{m},\mathbf{m}')\right] W_{AC}^{*}(\mathbf{m}',\mathbf{r}')$$
and $$\rho_{AC}^{-} = \frac{1}{2}\sum_{\mathbf{m},\mathbf{m}'} W_{AC}(\mathbf{m},\mathbf{r})\left[R_{AC}^{-}(\mathbf{m},\mathbf{m}')\right] W_{AC}^{*}(\mathbf{m}',\mathbf{r}') \tag{39}$$

Using Eq. (15), we can write;

$$\frac{N}{2} = \sum_{\mathbf{m},\mathbf{m}'} R_{AC}^{+}(\mathbf{m},\mathbf{m}') \int W_{AC}^{+}(\mathbf{m},\mathbf{r})\, W_{AC}^{+*}(\mathbf{m}',\mathbf{r})\, d\mathbf{r}$$
$$\frac{N}{2} = \sum_{\mathbf{m},\mathbf{m}'} R_{AC}^{+}(\mathbf{m},\mathbf{m}') = V_{oa} \sum_{\mathbf{m}} \int_{AC^{+}} d\mathbf{V}_k = N V_{oa} V_{AC}^{+} \tag{40}$$

So that;

$$V_{AC}^{+} = \frac{1}{4V_{oa}} \tag{41}$$

similarly;

$$V_{AC}^{-} = \frac{1}{4V_{oa}} \tag{42}$$

Using Eqs. (1), (5) and (36), the expressions for $R_{AC}^{+}(\mathbf{m},\mathbf{m}')$ and $R_{AC}^{-}(\mathbf{m},\mathbf{m}')$ are derived as;

$$R_{AC}^{+}(\mathbf{m},\mathbf{m}') = \frac{2}{N}\left[\sum_{\mathbf{k}}^{\mathbf{k}_{AC}^{+}} \exp(2\pi i\mathbf{k}.(\mathbf{m}-\mathbf{m}'))\,(1+\exp(-2\pi i\mathbf{K}.\mathbf{m}))+ \exp(2\pi i\mathbf{K}.\mathbf{m})+\exp(2\pi i\,\mathbf{K}.(\mathbf{m}-\mathbf{m}'))\right] \tag{43}$$

and

$$R_{AC}^{-}(\mathbf{m},\mathbf{m}') = \frac{2}{N}\left[\sum_{\mathbf{k}}^{\mathbf{k}_{AC}^{-}} \exp(2\pi i\mathbf{k}.(\mathbf{m}-\mathbf{m}'))\,(1-\exp(-2\pi i\mathbf{K}.\mathbf{m}))+ \exp(2\pi i\mathbf{K}.\mathbf{m})+\exp(2\pi i\,\mathbf{K}.(\mathbf{m}-\mathbf{m}'))\right] \tag{44}$$

Computational details

Wigner [1,2] observed that, "for sufficiently large r_s (low density limit), the wave function for the crystallized electrons should be a Gaussian". Thus, we have selected a single Gaussian of the form.

$$\varphi(r) = \left(\frac{2\alpha}{\pi}\right)^{1/2} \exp(-\alpha r^2) \tag{45}$$

where α is the variational parameter. The Wannier function is obtained as the linear combination of symmetrically orthonormalized Gaussian as indicated in Eq. (1). The reciprocal square root of the overlap matrix $\Delta^{-1/2}(\mathbf{m},0)$ {Eq. (2)} is computed using the procedure given by Calais and Appel [19]. We then minimize the energy functional.

$$\varepsilon = \int W^{*}(\mathbf{r}) H_{eff} W(\mathbf{r}) d\mathbf{r} \tag{46}$$

The orbital exponent of the Gaussian α is used as the variational parameter. The Hartree-Fock ground state energy values are found by extremizing the above functional.

The correlation energy is calculated from the Wigner Interpolation formula [1,2].

$$\varepsilon_c = -\frac{0.88}{r_s + 7.8} \tag{47}$$

The correlation energy calculated from the above equation is added to the Hartree-Fock ground state energy. In this way the ground state energy of the non-magnetic, ferromagnetic and antiferromagnetic phases of the 3D Wigner electron crystal corresponding to the hcp structure are computed.

Results and discussion

The ground state energies are computed for the non-magnetic, ferromagnetic and antiferromagnetic phases of the 3D Wigner electron crystal with a hcp structure corresponding to cubic and spherical surfaces as the region of occupation in k- space respectively with uniform neutralizing and Yukawa type positive backgrounds and are presented in **Tables 1** and **2** for r_s = 10 to 100.

Table 1 Electron crystal energy with a uniform neutralizing positive background (Ryd.).

r_s	Non-magnetic phase		Ferromagnetic phase		Antiferromagnetic phase	
	cubic	spherical	cubic	spherical	cubic	spherical
10	-0.12870	-0.13965	-0.25949	-0.26319	-0.08968	-0.13162
15	-0.10201	-0.11069	-0.19013	-0.25080	-0.07448	-0.10314
20	-0.08328	-0.09033	-0.14923	-0.18474	-0.06215	-0.08389
30	-0.06043	-0.06553	-0.10480	-0.12841	-0.04608	-0.06070
50	-0.03888	-0.04211	-0.06558	-0.08042	-0.03012	-0.03895
100	-0.02049	-0.02217	-0.03387	-0.04125	-0.01608	-0.02051

Table 2 Electron crystal energy with a Yukawa type positive background (Ryd.).

r_s	Non-magnetic phase		Ferromagnetic phase		Antiferromagnetic phase	
	cubic	spherical	cubic	spherical	cubic	spherical
10	-0.24356	-0.26110	-0.42638	-0.43749	-0.34465	-0.35362
15	-0.16920	-0.18120	-0.27271	-0.28730	-0.24056	-0.25906
20	-0.12970	-0.13848	-0.22276	-0.23418	-0.18228	-0.20101
30	-0.08807	-0.09383	-0.15031	-0.15847	-0.12504	-0.13815
50	-0.05319	-0.05669	-0.09058	-0.09566	-0.07559	-0.08381
100	-0.02591	-0.02757	-0.04464	-0.04719	-0.03712	-0.04136

From **Tables 1** and **2**, it is found that the ground state energy of a spherical surface as the region of occupation in k-space is less than a cubic surface for NC, FC and AC cases. The Yukawa type positive background leads to a lower ground state energy.

To evaluate the critical density for the Wigner transition, the electron crystal energies obtained with Yukawa type positive background with a spherical surface as the region of occupation in k-space are plotted against the density parameter r_s for non-magnetic, ferromagnetic and antiferomagnetic phases in **Figures 1 - 3**.

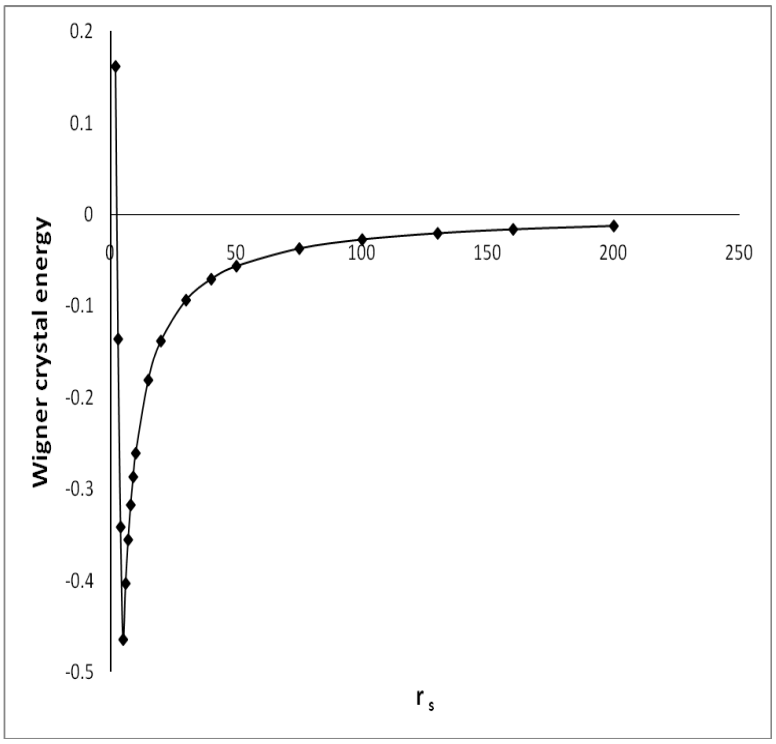

Figure 1 Electron crystal energy versus r_s - non-magnetic phase.

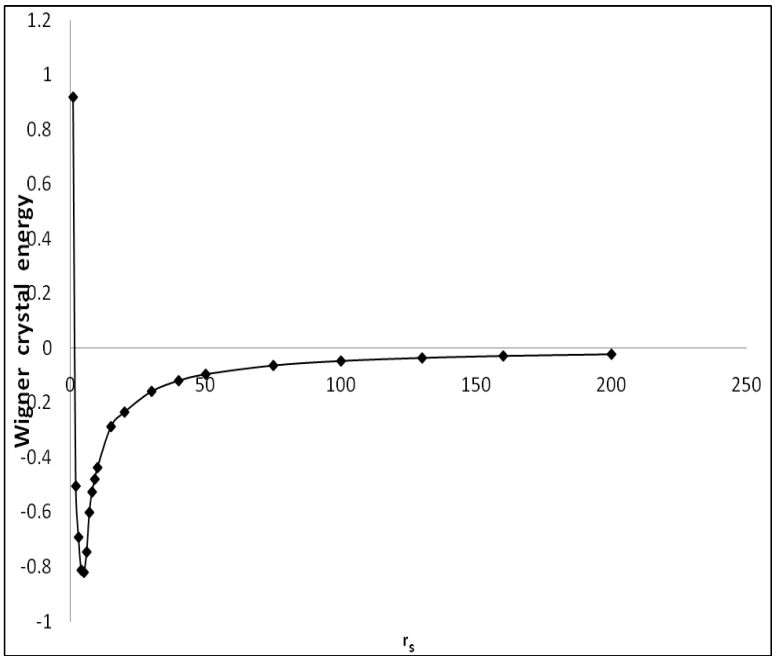

Figure 2 Electron crystal energy versus r_s - ferromagnetic phase.

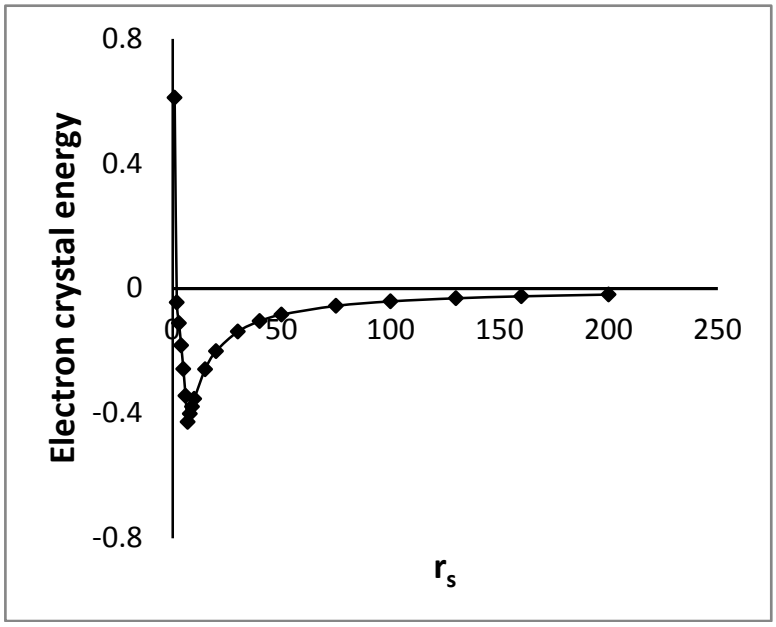

Figure 3 Electron crystal energy versus r_s - antiferromagnetic phase.

These figures are similar to the graph obtained by Carr [8] and Herring [26]. From **Figure 1**, it is found that for the non-magnetic case, the electron crystallization is above $r_s = 20$, which corresponds to a density of 2.03×10^{20} per cm^3 and the Wigner crystal is stable in this limit. For the ferromagnetic phase, **Figure 2**, it is found that the electron crystallizes out in the ferromagnetic phase at $r_s = 15.0$ corresponding to a density of 4.8×10^{20} per cm^3. From **Figure 3**, it is found that for the antiferromagnetic case, the discontinuous decrease of slope is above $r_s = 10$ corresponding to a density of 1.62×10^{21} per cm^3. This is an indication of a Wigner transition.

Table 3 Crystallization density of 3D Wigner electron crystal (electrons per cm^3).

Non-magnetic phase	Ferromagnetic phase	Antiferromagnetic phase
2.03×10^{20}	4.8×10^{20}	1.62×10^{21}
2.03×10^{20} [7]	2.53×10^{21} [3]	1.62×10^{21} - 2.53×10^{21} [3]
1.3×10^{23} [8]	1.62×10^{21} [5]	
2.0×10^{18} - 2.0×10^{19} [27]	7.0×10^{19} [9]	
2.03×10^{20} [28]	2.0×10^{18} [10]	
1.56×10^{19} - 1.62×10^{21} [29]	1.93×10^{23} [30]	
8.24×10^{19} [32]	2.36×10^{22} [31]	

The crystallization density calculated for the non-magnetic, ferromagnetic and antiferromagnetic phases of 3D Wigner electron crystal are compared with other experimental [9,27] and theoretical results [3,5,7,8,28-32] in **Table 3**. Our computed electron density value for non-magnetic phase is in agreement with that of Mott [7] and Nozieres and Pines [28]. It is found that the result obtained for antiferromagnetic case is in agreement with the results of Edwards and Hillel [3].

Conclusions

The ground state energies are computed for the non-magnetic, ferromagnetic and antiferromagnetic phases of the 3D Wigner electron crystal with a hcp structure corresponding to cubic and spherical surfaces as the region of occupation in k-space respectively with uniform neutralizing and Yukawa type positive backgrounds. It is found that the ground state energy of a spherical surface as the region of occupation in k-space is less than a cubic surface. The Yukawa type positive background leads to a lower ground state energy. The crystallization density of the non-magnetic, ferromagnetic and antiferromagnetic phases are 2.03×10^{20} cm^{-3}, 4.8×10^{20} cm^{-3} and 1.62×10^{21} cm^{-3}, respectively. The computed values are in agreement with other experimental and theoretical results. The ground state energy of the ferromagnetic phase is lower than that of the non-magnetic and antiferro-magnetic phases. Thus, at lower densities the ground state of the electron crystal is ferromagnetic.

Acknowledgements

We thank our college management for their constant encouragement. Financial assistance from UGC (MRP. F. No-38-141/2009), India is duly acknowledged with thanks.

References

[1] EP Wigner. On the interaction of electrons in metals. *Phys. Rev.* 1934; **46**, 1002-11.
[2] EP Wigner. Effects of the electron interaction on the energy levels of electrons in metals. *Trans. Faraday Soc*. 1938; **34**, 678-85.
[3] SF Edwards and AJ Hillel. Crystallization and magnetic ordering of an electron gas. *J. Phys*. 1968; **1**, 61-81.
[4] L Hedin. New method for calculating the one-particle Green's function with application to the electron-gas problem. *Phys. Rev*. 1965; **139**, A796-A823.
[5] S Misawa. Ferromagnetism of an electron gas. *Phys. Rev*. 1965; **140**, A1645-A1648.
[6] M Gell-Mann and KA Brueckner. Correlation energy of an electron gas at high density. *Phys. Rev*. 1957; **106**, 364-8.
[7] NF Mott. The transition to the metallic state. *Phil. Mag*. 1961; **B6**, 287-309.
[8] WJ Carr. Energy, specific heat and magnetic properties of the low-density electron gas. *Phys. Rev*. 1961; **122**, 1437-46.
[9] P Young, D Hall, ME Torelli, Z Fisk, JL Sarrao, JD Thompson, HR Ott, SB Oseroff, RG Goodrich and R Zysler. High temperature weak ferromagnetism in a low density free electron gas. *Nature* 1999; **397**, 412-4.
[10] DM Caperley. Return of the itinerant electron. *Nature* 1999; **397**, 386-7.
[11] S Zhang and DM Ceperley. Hartree-Fock ground state of the three-dimensional electron gas. *Phys. Rev. Lett*. 2008; **100**, Article ID: 236404.
[12] O Poplavskyy, MO Goerbig and CM Smith. Local density of states of electron-crystal phases in graphene in the quantum hall regime. *Phys. Rev. B* 2009; **80**, Article ID 195414.
[13] SS Shaimeev, VA Gritsenko and H Wong. Wigner crystallization due to electrons localized at deep traps in two-dimensional amorphous dielectric. *Appl. Phys. Lett*. 2010; **96**, Article ID 263510.
[14] CJ Campbell, AG Radnaev and A Kuzmich. Wigner crystals of ^{229}Th for optical excitation of the nuclear isomer. *Phy. Rev. Lett*. 2011; **106**, Article ID 223001.
[15] K Iyakutti, VJ Surya, R Rajeswarapalanichamy and Y Kawazoe. Wigner crystallization of quadratically dispersing electrons in graphene. *Int. J. Quantum Chem*. 2012; **112**, 1725-36.
[16] GF Koster. Localized functions in molecules and crystals. *Phys. Rev*. 1953; **89**, 67-77.

[17] W Kohn. Wannier functions and self-consistent metal calculations. *Phys. Rev. B* 1974; **10**, 382-3.
[18] PO Lowdin. Quantum theory of cohesive properties of solids. *Adv. Phys.* 1956; **5**, 1-171.
[19] JL Calais and K Appel. Inversion of cyclic matrices. *J. Math. Phys.* 1964; **5**, Article ID 1001.
[20] K Iyakutti and JL Calais. Electron crystallization using localized representation. *Pramana J. Phys.* 1990; **34**, 133-49.
[21] L Piela and J Delhalle. An efficient procedure to evaluate long range coulombic interactions within the framework of LCAO-CO method for infinite Polymers. *Int. J. Quantum Chem.* 1978; **13**, 605-17.
[22] J Delhalle, L Piela, JL Bredas and JM Andrei. Multipole expansion in tight-binding Hartree-Fock calculations for infinite model polymers. *Phys. Rev.* 1980; **B22**, 6254-67.
[23] HJ Monkhoest and NA Schwalm. Electrostatics for periodic films of atoms. *Phys. Rev*. 1981; **B23**, 1729-42.
[24] I Shavift. *Methods in Computational Physics.* vol. II. Academic Press, London, 1963, p. 30.
[25] EG Larson and WR Thorson. Model of electron correlation in solids. *J. Chem. Phys*. 1966; **45**, 1539-54.
[26] C Herring. *Magnetism*. vol. IV. Academic Press, London, 1966, p. 21.
[27] RS Crandall and R Williams. The structure of crystallized suspensions of polystyrene spheres. *Phys. Lett*. 1974; **48A**, 225-6.
[28] P Nozieres and D Pines. Correlation energy of a free electron gas. *Phys. Rev*. 1958; **111**, 442-54.
[29] FWD Wette. Note on the electron lattice. *Phys. Rev*. 1964; **135**, A287-A294.
[30] AK Rajagopal and SD Mahanti. Ferromagnetism of an electron gas. *Phys. Rev*. 1967; **158**, 353-5.
[31] Y Osaka. Note on the instability of an interacting electron gas in the *RP* approximation. *J. Phys. Soc. Japan* 1967; **22**, 1513-4.
[32] HMV Horn. Instability and melting of the electron solid. *Phys. Rev*. 1968; **157**, 342-9.